Effects of Asian air pollution transport and photochemistry on carbon monoxide variability and ozone production in subtropical coastal south China

C. Y. Chan, L. Y. Chan, K. S. Lam, and Y. S. Li

Environmental Engineering Unit, Department of Civil and Structural Engineering, Hong Kong Polytechnic University, Hong Kong, China

J. M. Harris and S. J. Oltmans

NOAA Climate Monitoring and Diagnostics Laboratory, Boulder, Colorado, USA

Received 5 January 2002; revised 19 July 2002; accepted 22 July 2002; published 18 December 2002.

[1] Surface ozone and carbon monoxide (CO) measured from a relatively remote coastal station in Hong Kong are analyzed to study the effects of pollutant transport and associated ozone production on CO and ozone variations in the subtropical south China region. CO and ozone concentrations show a common minimum in summer and in the maritime air masses from the South China Sea and Pacific Ocean. They have higher values in other seasons and in the continental air masses that have passed over mainland Asia and the East Asian coast. CO shows the maximum monthly median of 457–552 ppbv in winter while ozone shows a maximum of 40–50 ppbv in autumn and a distinct peak of 41–43 ppbv in spring. The CO concentrations especially in the continental air masses (median of 277 to 428 ppbv) are very high when compared with measurements in most parts of the world. This suggests that the south China region is under the strong influence of pollutant transport from the Asian continent and East Asian coast. Ozone and CO show strong positive correlations in the polluted maritime air masses and from late spring to early autumn (May–September) with the linear regression slopes of the ozone-CO plot from 0.08 to 0.22 (with respective standard errors from 0.01 to 0.03). The strong correlations and slopes plus the high CO levels indicate that there is substantial ozone production from pollution in the polluted maritime air masses and in the late spring to early autumn period. *INDEX TERMS:* 0345 Atmospheric Composition and Structure: Pollution—urban and regional (0305); 0368 Atmospheric Composition and Structure: Troposphere—constituent transport and chemistry; 0317 Atmospheric Composition and Structure: Chemical kinetic and photochemical properties; *KEYWORDS:* air pollution transport, photochemistry and ozone production

Citation: Chan, C. Y., L. Y. Chan, K. S. Lam, Y. S. Li, J. M. Harris, and S. J. Oltmans, Effects of Asian air pollution transport and photochemistry on carbon monoxide variability and ozone production in subtropical coastal south China, *J. Geophys. Res.*, *107*(D24), 4746, doi:10.1029/2002JD002131, 2002.

1. Introduction

[2] The East Asia region is a large source of anthropogenic air pollutant emissions. There has been a growing concern about the impacts of Asian emissions on the atmospheric chemical evolution in the western Pacific Rim, global atmosphere [*Berntsen et al.*, 1996; *Hoell et al.*, 1997; *Jacob et al.*, 1999] and the deterioration of air quality in the region [*Chan and Chan*, 2000]. Export of pollutants from Asia into the central Pacific and northeast Asian Pacific atmosphere has been well established [*Merrill*, 1989; *Uematsu et al.*, 1983; *Crawford et al.*, 1997; *Newell et al.*, 1997]. *Newell et al.* [1997] pointed out that Asian pollutants have an influence on the global atmosphere as they may enter the stratosphere. Recently, transport of Asian pollution to North America has been reported [*Jaffe et al.*, 1999; *Jacob et al.*, 1999]. *Jaffe et al.* [1999] showed that transport of Asian air pollution to North America has a significant impact on the concentration of a large number of atmospheric species in the air arriving in North America. *Jacob et al.* [1999] also discussed the effect of rising Asian emissions on surface ozone in the United States. *Yienger et al.* [2000] reported that pollutant transport from Asia to North America could be episodic in nature.

[3] However, the impacts of Asian pollutant emissions on subtropical south China region are less well known. The subtropical south China region includes the fast growing Pearl River Delta region in Guangdong Province, Hong Kong and Taiwan (Figure 1). The geographical location puts south China as a receptor of the anthropogenic emissions from the Asian continent and Southeast Asia [*Chan et al.*, 1998a]. *Chan et al.* [1998a, 1998b] proposed that the changes of prevalent maritime and continental air mass flow are important factors governing the variation of surface ozone in Hong Kong. *Buhr et al.* [1996] and *Wang et al.*

0148-0227/02/2002JD002131

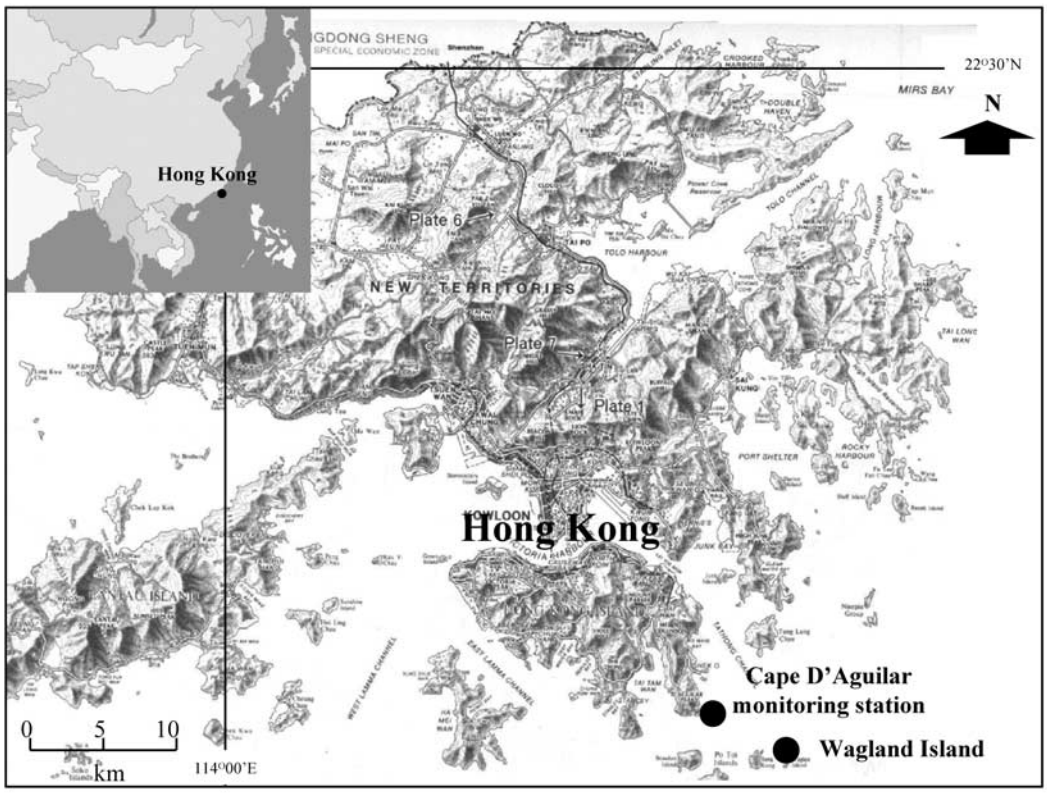

Figure 1. Geographical locations of Hong Kong and the Cape D'Aguilar monitoring station. See color version of this figure at back of this issue.

[1997] revealed through trace gas measurements in southern Taiwan and Hong Kong respectively that high levels of trace gases are associated with continental outflows reaching south China and Hong Kong. *Chan and Chan* [2000] found that the background outflow of Asian pollutants can be significantly modified on their way to the Pacific Ocean when passing through the industrialized and urbanized south China region. In this study we present surface ozone and CO concentrations measured from a relatively remote monitoring station in Hong Kong. The aim is to study the effects of Asian pollution transport on variability of CO and ozone, and the seasonal variation of photochemical ozone production in the south China region.

2. Ozone and Carbon Monoxide Measurement

[4] Surface ozone and CO measurements began in late 1993 at the Hong Kong Polytechnic University Background Air Quality Monitoring Station. Figure 1 shows the geographical location of the station. The station is located at Cape D' Aguilar (22.2°N, 114.3°E) and is situated at the top of a cliff at 60 meters above mean sea level. The site is primarily a rural area relatively remote from domestic pollutants emitted from metropolitan Hong Kong. It is situated at the southeastern tip of Hong Kong Island and bounded by the sea from northeastern to southeastern direction. A detailed description of the station, sampling line, CO and ozone measuring methods together with quality control and assurance procedures has been given by *Chan et al.* [1998a].

[5] In this study, we focus on the hourly ozone and CO data from January 1994 to December 1996. The data were derived from 1-minute averaged raw data. The annual ozone capture rates were 79% in 1994, 94% in 1995 and 96% in 1996. The respective rates for CO were 77%, 93% and 84%. The data capture rates in August 1994 were lower than 25% due to a major break down of the station. The CO and ozone data with corresponding hourly surface wind speed lower than 3 m/s measured on Waglan Island (Figure 1) were excluded. This is because when below this wind speed, our station may be affected by the pollutants emitted from the village nearby. The wind measured on Waglan Island is considered to represent the prevailing wind as the station is away from any geographical barrier. The above screening processes sorted out around 26% of ozone and 25% of CO data.

3. Back Air Trajectory and Cluster Analysis

[6] The trajectories used in this study are from the Climate Monitoring and Diagnostics Laboratory, the National Oceanic and Atmospheric Administration of the USA. They are calculated by the trajectory model described by *Harris and Kahl* [1994] using the meteorological input and topography data from the European Centre for Medium Range Weather Forecasts. In this model air parcels are assumed to move dry adiabatically along isentropic surfaces. The model calculates two 10-day back air trajectories daily at 00 and 12 UT (0800 and 2000 Hong Kong time) together with altitude, pressure and temperature at each point. The input data has a spatial resolution of 2.5 degree and a temporal resolution of 12 hours. The trajectories from the model are believed to give a reasonable representation of the large-scale circulation motion. They can be used to identify the source region of

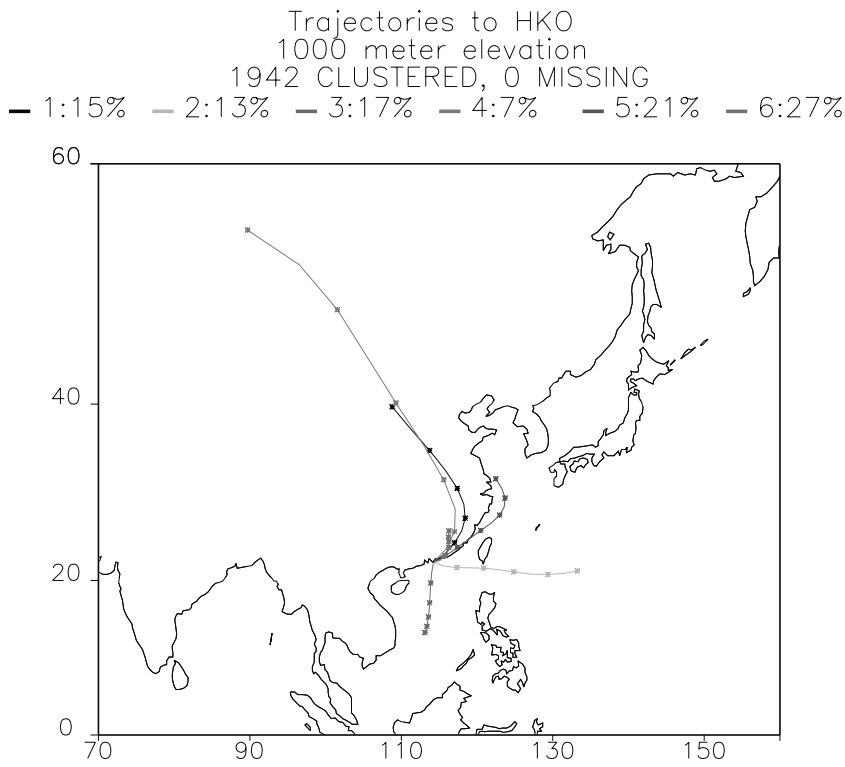

Figure 2. The six mean trajectory clusters arriving at Hong Kong. See color version of this figure at back of this issue.

pollutants [*Harris and Kahl*, 1994], although the specific origin of an air parcel cannot be exactly determined.

[7] We employed cluster analysis as described by *Harris and Kahl* [1990] to apportion the trajectories into groups and clusters. The criterion used to identify each cluster is a mathematical algorithm, which groups similar trajectories into clusters while trying to maintain distinctions among the clusters. The trajectories are classified into six clusters. Our experience shows that six clusters do show enough detail while summarizing the different pathways succinctly. Thus the clusters are determined in an objective way, which maximizes the differences in trajectories between clusters while minimizing the differences in trajectories within each cluster. These clusters represent the average trajectory within a group of trajectories of similar shape and length. Figure 2 presents the six major cluster means derived from a total of 1944 trajectories from 1994 to 1996. The cluster means are marked to indicate the 1-day upwind interval for the 5 days backward. The numbers at the ends of the mean trajectories show the cluster identifiers. The percentages of trajectories that occur in the cluster are also shown. Figure 3 shows typical 10-day back trajectories of the six cluster means. These typical trajectories are shown in order to illustrate more clearly the vertical motions of the associated air masses. Table 1 summarizes the monthly frequency distribution of the trajectories.

4. Results and Discussion

4.1. CO and Ozone Concentration in the Air Masses

4.1.1. CO and Ozone Concentrations in Maritime Air Masses

[8] To assess the origin of pollution and its transport to the south China region, we use isentropic back air trajectories in conjunction with CO and ozone concentrations to characterize the prevalent air masses reaching Hong Kong. We only considered those homogeneous air masses with the same trajectory cluster type at 00 and 12 UTC. The ozone and CO data in those days with transition air trajectories were discarded. Table 2 summarizes the distributions of the ozone and CO concentrations associated with the six clusters. Included in this table are also the number of days and hours of the data in each trajectory cluster.

[9] The air masses associated with clusters 2 (T2) and 3 (T3) are maritime origin from the middle Pacific and the South China Sea respectively flowing in a general southwest to east direction to the south China region. Examination of the individual trajectory (Figure 3) revealed that the air masses originate and have spent a long time within the marine boundary of the middle northern Pacific and equatorial Pacific. The trajectories associated with these two clusters accounted for 13 and 17% of the total trajectories. They occur mostly from mid spring (March) to mid autumn (September) and especially in summer (June to August). The median ozone associated with cluster 2 and 3 are 21 and 13 ppbv respectively. The respective values for CO are 135 and 105 ppbv. The ozone and CO concentrations in the air masses associated with these two trajectory clusters are very similar. However, from Table 2 we see that the air mass associated with cluster 2, which flows from central northern Pacific through the nearby vicinity of Taiwan Island, has higher CO and ozone burden when compared with its counterpart from the South China Sea. This may reflect the fact the air mass from the central northern Pacific sometimes has to pass over the large emission source region of southern Taiwan Island and the eastern coast of south China as revealed by individual trajectory. The median ozone concentrations associated with

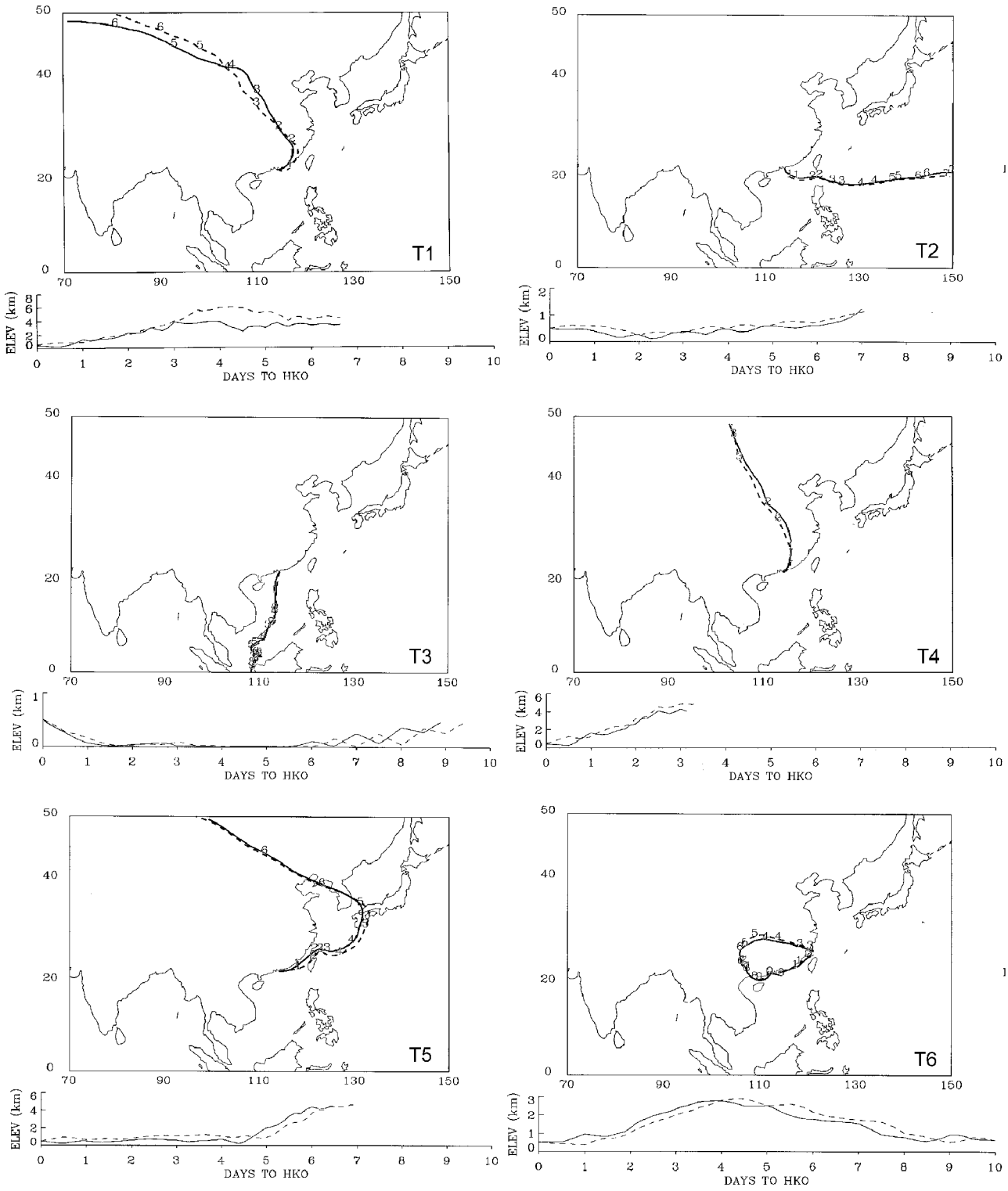

Figure 3. Typical trajectories of the six mean trajectory clusters.

maritime air masses from the central Pacific and the South China Sea measured at Cape D'Aguilar in summer (21 and 13 ppbv respectively) are comparable in magnitude to those observed at Oki, Okinawa of Japan (11–15 and 22 ppbv respectively) and Kenting of Taiwan (9 and 18 ppbv respectively) [*Akimoto et al.*, 1996; *Buhr et al.*, 1996].

4.1.2. CO and Ozone Concentration in Continental Air Masses

[10] The air masses associated with cluster 1 (T1), 4 (T4), 5 (T5) and 6 (T6) are continental in nature from the Asian mainland flowing in a general northwest to northeast directions to reach the south China region. They account

Table 1. Monthly Frequency Distribution of the Mean Trajectories in Each Cluster (1994–1996)[a]

	Trajectory Type						
	1	2	3	4	5	6	Total
Jan	42 (2.2)	4 (0.2)	0 (0.0)	18 (0.9)	17 (0.9)	105 (5.4)	186
Feb	42 (2.2)	2 (0.1)	4 (0.2)	16 (0.8)	21 (1.1)	85 (4.4)	170
Mar	46 (2.4)	29 (1.5)	13 (0.7)	16 (0.8)	17 (0.9)	65 (3.3)	186
Apr	13 (0.7)	48 (2.5)	34 (1.7)	8 (0.4)	30 (1.5)	49 (2.5)	182
May	5 (0.3)	14 (0.7)	68 (3.5)	5 (0.3)	26 (1.3)	57 (2.9)	175
Jun	0 (0.0)	32 (1.6)	64 (3.3)	0 (0.0)	5 (0.3)	10 (0.5)	111
Jul	0 (0.0)	22 (1.1)	82 (4.2)	0 (0.0)	0 (0.0)	3 (0.2)	107
Aug	0 (0.0)	38 (2.0)	63 (3.2)	0 (0.0)	3 (0.2)	19 (1.0)	123
Sept	19 (1.0)	30 (1.5)	8 (0.4)	0 (0.0)	68 (3.5)	27 (1.4)	152
Oct	30 (1.5)	16 (0.8)	2 (0.1)	8 (0.4)	115 (5.9)	15 (0.8)	186
Nov	44 (2.3)	11 (0.6)	0 (0.0)	31 (1.6)	64 (3.3)	30 (1.5)	180
Dec	42 (2.2)	8 (0.4)	0 (0.0)	29 (1.5)	42 (2.2)	65 (3.3)	186
Total	283 (14.6)	254 (13.1)	338 (17.4)	131 (21.0)	408 (21.0)	530 (27.3)	1944

[a]The values are in percentage.

for 70% of the air parcels reaching Hong Kong. The transport patterns for cluster 1 and 4 show the strong and fast outflow of the continental air masses directly to the south China region. They occur mainly from late autumn to mid spring. The characteristics of the air masses associated with these two clusters are similar. The only difference is that the later air mass moves faster. Trajectory 5 shows a modified continental air mass transported along the East Asian coast over the boundary of Asian continent and western Pacific to reach the south China region. This transport pattern occurs mainly from autumn to early winter. Cluster 6 shows the local looping of air mass in the south China region. This transport pattern occurs predominately from December to May. Notably, the air masses associated with these trajectories very often show significant descending motion from the lower free troposphere to the boundary layer during the transport from the high latitudes to the south China region (Figure 3).

[11] The median CO levels in the continental air masses range from 277 to 428 ppbv. The local looping air mass is the most polluted with the highest median CO concentration of 428 ppbv (Table 2). The CO concentration (277 ppbv) in the modified continental air mass (T5) is the lowest among the continental air masses. This is because the air pollutants in the continental air are diluted by the oceanic air mass from the East Asian coast. The median ozone concentration in the continental air masses ranges from 35 to 46 ppbv with the highest concentrations in the fast-moving and pure continental air masses (T1 and T4). The local looping air mass (T6) has the lowest ozone concentration of 35 ppbv.

4.2. Effects of Asian Pollution Transport on Seasonal CO and Ozone Variability in South China

[12] The impacts of Asian pollution in south China are clearly reflected by the measurements at Cape D'Aguilar. Figure 4a shows the monthly distribution of CO concen-

Table 2. Distribution of Ozone and CO Concentrations in Each Trajectory Clusters[a]

	Concentration of Ozone, ppbv					
Trajectory Type	1	2	3	4	5	6
No. of days	63	69	92	33	114	143
No. of O_3-hours	939	1141	1117	523	1842	1891
Maximum	85	162	81	75	76	85
99 percentile	75	52	55	68	71	72
95 percentile	64	47	44	59	61	60
90 percentile	60	43	33	57	56	55
75 percentile	52	35	20	52	49	46
50 percentile	45	21	13	46	42	35
25 percentile	38	13	9	38	35	22
5 percentile	18	7	4	29	17	10
1 percentile	9	4	1	17	11	2
	Concentration of CO, ppbv					
Trajectory Type	1	2	3	4	5	6
No. of days	61	71	82	33	99	140
No. of O_3-hours	835	1141	971	523	1642	1844
Maximum	1453	1239	942	718	1124	1799
99 percentile	840	621	468	625	881	911
95 percentile	728	477	321	500	575	769
90 percentile	635	338	258	479	469	685
75 percentile	504	228	148	432	364	554
50 percentile	403	135	105	367	277	428
25 percentile	285	90	84	301	220	307
5 percentile	208	67	66	240	168	179
1 percentile	173	57	58	186	142	82

[a]Based on the trajectory clusters with same trajectory type at 00 and 12 UTC.

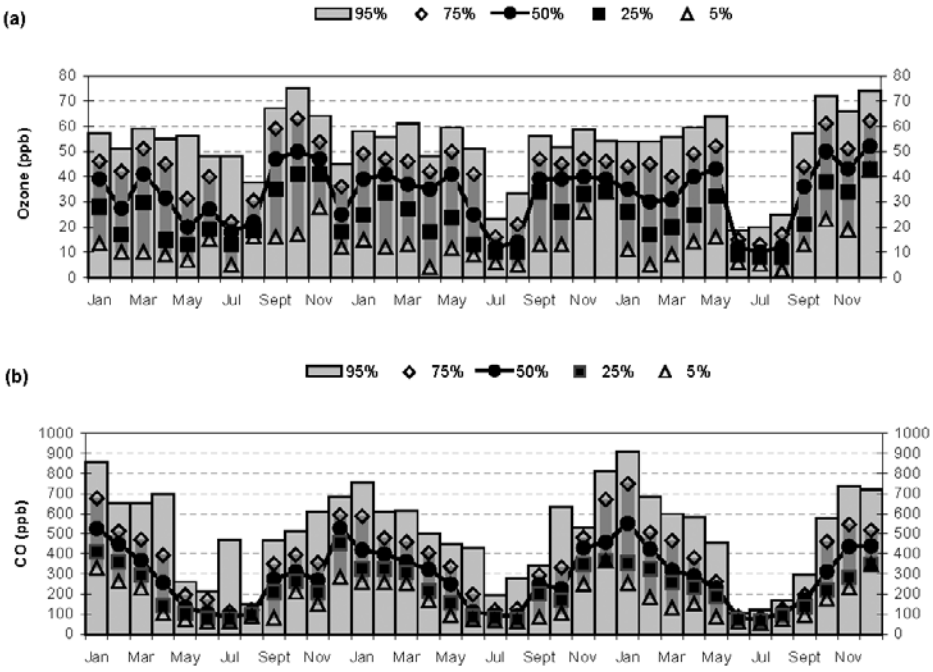

Figure 4. Monthly distribution of (a) ozone and (b) CO concentrations at Cape D'Aguilar from 1994 to 1996. The data include all data with corresponding wind speed greater than 3 m/s.

trations observed from 1994 to 1996. CO in air is mainly emitted from human sources associated with fuel combustion and it has a fairly long lifetime in the atmosphere. Its relative concentration level can thus be used as a tracer of anthropogenic impact on the natural atmosphere [*Parrish et al.*, 1993]. The annual mean CO concentrations at Cape D'Aguilar range from 306 ppbv in 1994 to 301 ppbv in 1996. The variation of CO shows a consistent seasonal cycle with a minimum in summer. CO shows a sharp increase in autumn until it reaches the maximum in middle winter (January). It then decreases substantially through spring to the minimum. The monthly median CO concentrations showed the maximum in December or January (457 to 552 ppbv) and the minimum in July of 1994 (89 ppbv), July of 1995 (92 ppbv) and June of 1996 (74 ppbv). CO shows greater variation in autumn, winter and spring and the mean CO concentrations are consistently low in summer.

[13] The CO concentration levels observed at Cape D'Aguilar, especially in autumn, winter and spring accompanying the continental air masses are very high when compared with the background measurements in Europe, Northern America and the mid latitudes of East Asian Pacific Rim. *Derwent et al.* [1998] reported the mean CO concentrations of the Northern Hemisphere mid-latitude background air to be 125 ± 27 ppbv at Mace Head. *Parrish et al.* [1998] reported an annual mean and median average of 141 ppbv and 136 ppbv at Sable Island, North Atlantic. The measurements at Niwot Ridge, Colorado, in the USA observed an annual mean concentration of 123 ppbv. *Pochanart et al.* [1999] observed the monthly mean CO concentrations ranging from 105 to 248 ppbv at Oki, Japan. The respective values from the measurements at Happo, Japan range from 151 to 236 ppbv [*Kajii et al.*, 1998]. At Cape D' Aguilar, the monthly median CO concentrations ranged from 74 to 113 ppbv in summer and from 398 to 552 ppbv in winter. These facts suggest that the south China region including Hong Kong is under the strong influence of the anthropogenic burdens of the continental air masses from the Asian continent and East Asian coast.

[14] We noted that surface ozone variation in Hong Kong is not in phase with the anthropogenic indicator CO. Figure 4b shows the monthly distributions of ozone concentrations observed from 1994 to 1996. *Chan et al.* [1998a] noted that the seasonal surface ozone pattern in Hong Kong is quite unique, having a pattern different from that in the free troposphere, where ozone has a dominant springtime peak. Surface ozone has a summer minimum (12–27 ppbv), a distinct secondary peak in spring (37–45 ppbv) and a major peak in autumn (44–58 ppbv). Normally ozone shows a seasonal cycle with a dominant spring maximum similar to that in the free troposphere or lower stratosphere at the high and mid latitudes of Europe and North America. For example, *Derwent et al.* [1998] observed an ozone seasonal cycle with a springtime maximum and a winter minimum in the background air at Mace Head (53°N, 10°W). *Moody et al.* [1995] observed that the monthly average ozone off the coast of North America in Bermuda shows a peak in April and a distinct minimum during summer months. *Harris et al.* [1998] reported that surface ozone measured in Mauna Loa of Hawaii, central Pacific, has a maximum during springtime. In the remote areas of Japan, surface ozone measurements and in situ ozonesonde observations show a strong spring maximum and a summer minimum [*Ogawa and Miyata*, 1985, 1989; *Tsuruta et al.*, 1989; *Sunwoo et al.*, 1994; *Pochanart et al.*, 1999].

[15] The seasonal CO and ozone cycle is obviously a reflection of the changes of continental air mass flow from autumn to spring and the maritime air mass flow in summer.

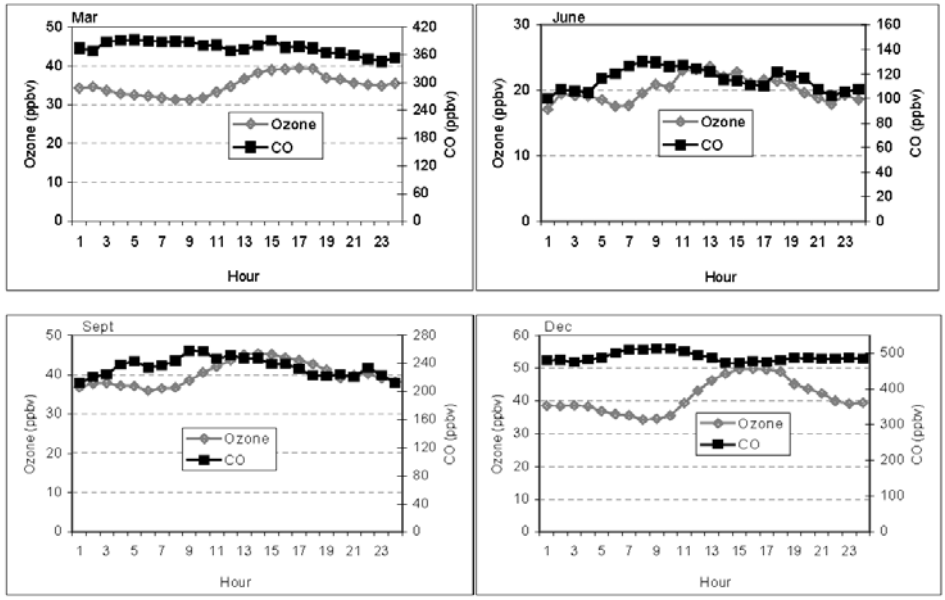

Figure 5. The diurnal variation of monthly average ozone and CO concentrations (ppbv) in March, June, September and December.

The tropical and equatorial marine air is well known to be low in pollutants and ozone [*Piotrowicz et al.*, 1986] since there is a lack of emission sources in the ocean as compared to the continent. The wide inflow of marine air masses in summer is considered as the major cause of low ozone and other trace gases concentrations in Japan [*Ogawa and Miyata*, 1985; *Tsuruta et al.*, 1989; *Sunwoo et al.*, 1994; *Pochanart et al.*, 1998; *Kajii et al.*, 1998] and Taiwan. The continental air mass from Asia has been shown to be rich in both natural and anthropogenic emission sources [*Akimoto et al.*, 1996; *Chan et al.*, 1998a]. This is because the air mass picks up a huge amount of pollutants from the large areas of the continental mainland and the highly industrialized and urbanized zones of the East Asian coastline on its way to the South China Sea. Owing to the large-scale downward motion associated with the winter monsoon, these pollutants are trapped in the shallow boundary layer [*Newell et al.*, 1997; *Chan and Chan*, 2000]. *Blake et al.* [1997] observed high concentrations of anthropogenic hydrocarbons and halocarbons in the continental outflow during the PEM-West B period. They also found that these pollutants are mainly observed at the low altitudes. *Talbot et al.* [1997] also reported similar observations for acidic gases. *Arimoto et al.* [1997] compared the trace constituents from ground stations and the aircraft measurements during PEM-West B mission. They found high concentrations of aerosol, ozone and CO at the Hong Kong ground station relative to the aircraft and concluded that much of the pollutant outflow from southeastern Asia occurs in the lower troposphere.

4.3. Ozone-Carbon Monoxide Relationship and Effects of Photochemistry on Seasonal Ozone Variability

[16] In order to reveal and quantify any possible relationship between CO and ozone, we performed correlation and linear regression analysis for the simultaneous CO and ozone data from 1994 to 1996. The correlation coefficient and the slope of the linear regression line were calculated using the ''least squares'' method. Before the analysis, we looked at the diurnal cycles of CO and ozone concentration in each month (Figure 5) and we found that there was a strong diurnal variation of ozone concentration. The variation may be due to the titration by local emissions and surface deposition under a tight boundary layer. The diurnal variation of CO concentration is less apparent but high concentrations were still noticeable at the morning (7:00–10:00 LST), probably reflecting the influence of local traffic. We thus performed the correlation and linear regression analysis based on the noontime (11:00–15:00 LST) CO and ozone data to minimize the possible titration and deposition effects. We found that the noontime data did give better correlation than the daily average CO and ozone data.

[17] Figure 6a shows the square of correlation coefficients (R^2) and slopes (m) based on the linear regression relationship between ozone and CO concentrations (i.e. $[O_3] = m[CO] + c$, where $[O_3]$ and [CO] are the averaged noontime ozone and CO concentration respectively, m is the slope and c is a constant) in each trajectory cluster. The ozone and CO concentrations in the maritime air masses from the central Pacific and the South China Sea have fairly strong correlations. The R^2 values are 0.40 and 0.53 respectively. The regression slopes of these air masses are 0.09 and 0.12 (with standard error of 0.01 and 0.02 respectively) respectively. In particular, the CO-ozone correlation is strong in the central Pacific air masses (T2), which had passed through the Taiwan Island and eastern part of south China. The square of correlation coefficient and the slope in this cluster in June reaches 0.88 and 0.28 (with a standard error of 0.01) respectively (Figure 6b).

[18] The R^2 values in the continental and modified continental air masses were very low and the regression slope, m, was always negative. We had also performed correlation and regression analysis for the noontime CO and ozone concentrations on monthly basis. Figure 7 shows the monthly

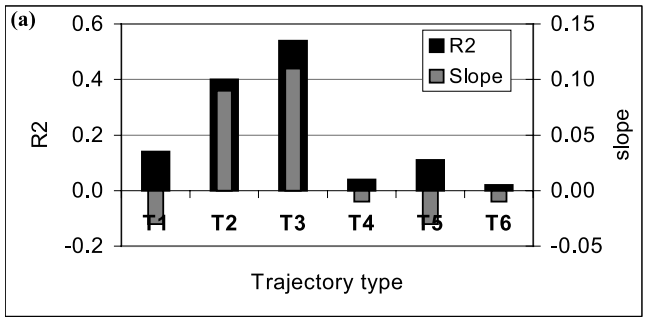

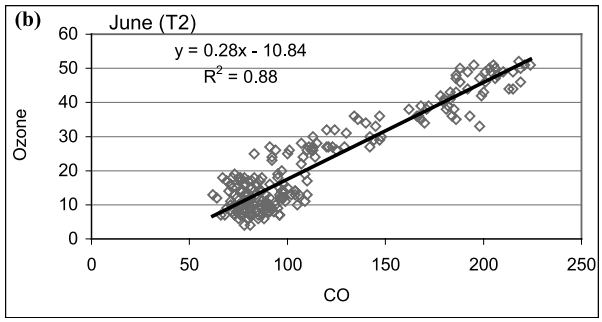

Figure 6. Distribution of slope of ozone-CO regression line (open cycle) and the square of correlation of coefficient (R^2) (a) in different trajectory clusters and (b) in trajectory cluster 2 (T2) in June calculated by linear regression analysis.

distributions of m and R^2 for the data from 1994 to 1996. These plots generally reflect the seasonal variation of m and R^2 in individual years. Figure 8 shows the scatterplots of CO-ozone concentrations in March, June, September and December for the noontime data to illustrate the CO-ozone correlations. These months were selected to represent the typical months of the four seasons. Strong and positive correlations are found especially from late spring to early autumn (May–September). The R^2 values are 0.34 in May, 0.83 in June, 0.86 in July, 0.58 in August and 0.50 in September. The R^2 values in June, July and August are statistically significant with confidence levels higher than 99%. The m values in these months range from 0.08 (standard error equals to 0.02) in May to 0.23 (standard error equals to 0.03) in August and have an average of 0.16. The respective values for June, July and September are 0.22, 0.16 and 0.10 (standard errors equal to 0.02, 0.01 and 0.02 respectively).

[19] The linear regression slope values observed from late spring to early autumn are consistent with those reported from the developed countries such as in the USA and Japan. *Chin et al.* [1994] reported that the aged Denver plume at Niwot Ridge, Colorado shows a strong ozone-CO correlation with a linear regression slope of 0.15. They also show that slopes of 0.3 to 0.4 are generally characteristic of North American sites. *Kajii et al.* [1998] observed the slopes 0.18 and 0.19 in April and May respectively at Happo, Japan. *Pochanart et al.* [1998] reported a similar value in the continental air mass at Oki, Japan. However, the slopes of ozone-CO plots in Hong Kong are lower than the ones measured at the three Canadian marine sites downwind of the United States reported by *Parrish et al.* [1993]. The readers are reminded that direct comparison on the photochemical activity with other sampling sites judging from slopes of linear regression may not be simple. This is because slope values strongly depend on level of CO concentration and that the CO concentration levels at Cape D'Aguilar are higher that those at other sampling sites.

[20] The low ozone (about 10 ppbv) and low CO levels (about 80 ppbv) observed in many of the samples suggest that photochemical ozone destruction dominates in clean maritime air masses (Figure 8). However, the strong correlation between ozone and CO data plus the high CO levels in the maritime air masses that pick up pollution from close passage to Taiwan suggest that there is still fairly high photochemical production of ozone from the anthropogenic ozone precursors in the inflow air masses that received recent injections of anthropogenic emissions. As the season progresses from late summer to early autumn (September), ozone production starts to dominate in the continental air that is rich in anthropogenic emissions. This is reflected by the sharp increase in ozone concentration along with CO concentration in August and September (Figure 4) and the high ozone-CO correlation (Figure 7). At the same time, fair weather gradually develops from late summer to early autumn with the inflow of polluted continental air to the south China region [*Chan et al.*, 1998a]. The ozone brought in by the continental air reaches the maximum concentration in autumn, when the atmospheric environment in south China is most favorable for ozone formation [*Chan et al.*, 1998a]. Our results are consistent with the results of *Davis et al.* [1996]. *Davis et al.* [1996] reported with a model computation result that the clean marine boundary layer air in the western Pacific produces significant negative ozone production potential and the fresh continental boundary layer air produces large positive values of ozone production potential. The transition of ozone from the peak to the lower level in winter, early or mid spring is due to the gradual slowdown of ozone production in the cold weather as the

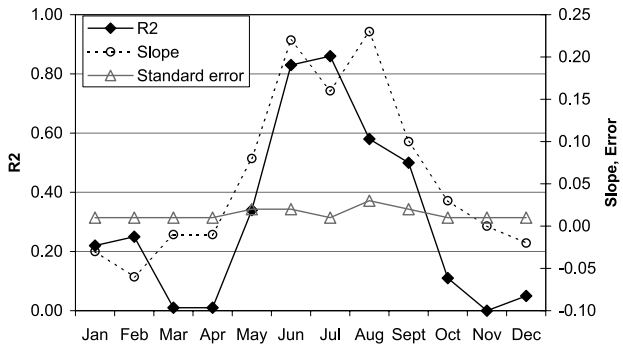

Figure 7. Monthly distribution of the slope of ozone-CO regression line (open cycle), the square of correlation of coefficient (R^2) (close cycle) and the standard errors of the slopes (triangles) calculated by linear regression analysis based on averaged noontime (11:00–15:00LST) data.

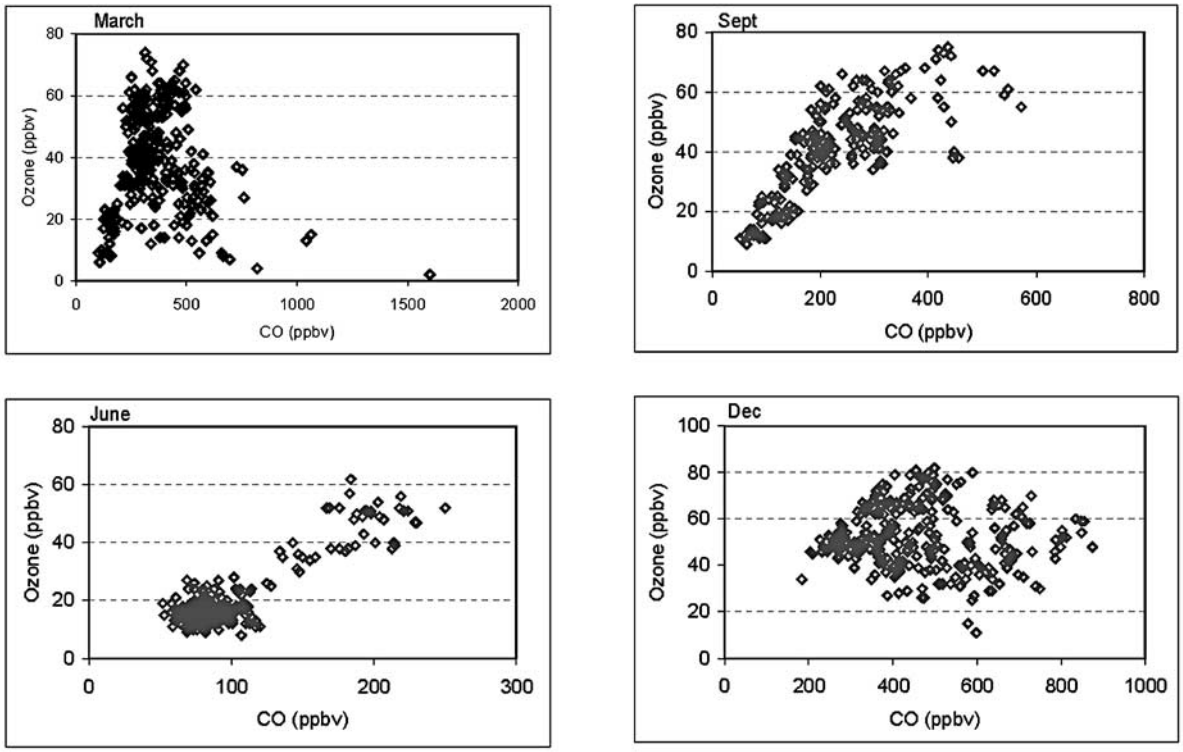

Figure 8. Scatterplots of hourly noontime (11:00–15:00LST) ozone and CO concentrations in March, September, June and December.

season progresses. This is because the decreases in temperature, daily global solar radiation and total bright sunshine together with low concentration of hydroxyl radicals in winter [*Kajii et al.*, 1998] limit the photochemical production of ozone.

[21] The secondary springtime ozone peak in Hong Kong is primarily the result of abrupt enhancements of photochemical production in the continental air masses, which bring in higher background ozone and high levels of pollutants. There is a gradual increase of temperature, solar radiation and sunshine hours in late spring and early summer. Also, there are alternating intrusions of the continental and marine air masses in late spring and early summer (Table 1). These conditions are expected to cause abrupt ozone production in the continental air masses and cause an overall high concentration ozone peak in spring. At the mid-latitudes of the Northern Hemisphere, stratospheric intrusion of ozone is thought to be the dominant cause of springtime tropospheric ozone maximum. In Japan, the springtime ozone maximum is usually attributed to significant contribution of the vertical stratospheric ozone intrusion to the ground level ozone. *Kato et al.* [1990], *Ueda and Carmichael* [1995] conducted field observations and performed numerical simulation for the observed springtime ozone episodes. They concluded that the combined effects of the photochemical ozone and the high background ozone of stratospheric origin are the causes of the episodes. We believe that the direct vertical stratospheric exchange is not the dominant source of the springtime surface ozone peak observed in Hong Kong. This is because the surface ozone in Hong Kong shows a different pattern from that in the free troposphere. Also, the boundary layer air in the south China region is isolated from the upper atmospheric air by the strong westerly flow in the troposphere [*Chan et al.*, 2000]. Chan et al. revealed through ozonesonde profiles that ozone concentration in the free troposphere in the springtime over Hong Kong is isolated from the local boundary layer by a strong temperature inversion at the top of the layer.

[22] It should however be pointed out that besides photochemistry, ozone transport also plays an important role influencing the ozone cycle observed at Cape D'Aguilar. Figure 3 shows that ozone-rich continental air masses are associated with substantial descending motion at around 3–6 days before reaching south China. This descending motion may have resulted in mixing of free tropospheric ozone with the anthropogenic ozone within the boundary layer during transport to south China and cause the general high ozone concentrations in the continental air mass flow season from autumn and spring. In fact, such transport of high ozone from the unpolluted upper troposphere has been found in proximity to the polluted eastern seaboard at Bermuda and Barbados of North America [*Oltmans and Levy*, 1992].

5. Conclusion

[23] In this paper, the surface CO and ozone measurements from a relatively remote coastal site in subtropical south China in Hong Kong are analyzed through the

interaction of transport patterns and the chemical relationships between ozone and CO. The major transport patterns of Asian pollution to Hong Kong are derived from the cluster analysis on isentropic trajectories. CO is used as a tracer of anthropogenic pollutant levels in each prevalent inflow air mass. The possible effects on photochemical production of ozone from the pollutants in the prevalent air masses is assessed through correlation and regression analysis of simultaneous ozone and CO data in each trajectory cluster and on monthly basis. Surface ozone shows a minimum in summer and a maximum in autumn. The winter and spring seasons are transition periods with a distinct secondary peak in spring. CO shows a relatively high concentration when compared with other measurements around the world, with a winter maximum and a summer minimum. This suggests that the south China region including Hong Kong is under the strong influence of anthropogenic emissions from the upwind Asian continent and the East Asian coast. The summer low ozone and CO concentrations are due to the predominant inflow of maritime air masses from the tropical central Pacific and the equatorial South China Sea. The higher ozone and CO concentrations in the other seasons are as a result of widespread outflow of continental air masses, which originate and have passed through the Asian mainland and east coast of Asia. Ozone and CO show strong correlations in the polluted maritime air masses and from late spring to early autumn suggesting that there is substantial ozone production from pollution in the polluted maritime air masses and in the late spring to early autumn period. Background maritime air masses have low CO and ozone. The strong correlation results from higher ozone and CO in maritime air masses are due to the fact that the air masses have been recently polluted during transport to the Hong Kong area. These suggest that besides air pollutant transport, the associated photochemical production of ozone also contributes to the seasonal variation of ozone in the subtropical and coastal south China region.

[24] **Acknowledgments.** This study is supported by a Hong Kong Polytechnic University research grant and a grant from the Research Grant Council of Hong Kong.

References

Akimoto, H., et al., Long-range transport of ozone in the East Asian Pacific Rim region, *J. Geophys. Res.*, *101*, 1999–2010, 1996.

Arimoto, R., R. A. Duce, J. M. Prospero, D. L. Savoie, R. W. Talbot, J. E. Dibb, B. G. Heikes, B. J. Ray, N. F. Lewis, and U. Tomza, Comparisons of trace constituents from ground stations and the DC-8 aircraft during PEM-West B, *J. Geophys. Res.*, *102*, 28,539–28,550, 1997.

Berntsen, T., I. S. A. Isaksen, W. C. Wang, and X. Z. Liang, Impacts of increased anthropogenic emissions in Asia on tropospheric ozone and climate-a global 3-D model study, *Tellus Ser. B*, *48*, 13–32, 1996.

Blake, N. J., D. R. Blake, T.-Y. Chen, J. E. Collins Jr., G. W. Sachse, B. E. Anderson, and F. S. Rowland, Distribution and seasonality of selected hydrocarbons and halocarbons over the western Pacific basin during PEM-West A and PEM-West B, *J. Geophys. Res.*, *102*, 28,315–28,331, 1997.

Buhr, M. P., K.-J. Hsu, C. M. Liu, R. Liu, L. Wei, T.-C. Liu, and Y.-S. Kuo, Trace gas measurements and air mass classification from a ground station in Taiwan during the PEM-West A experiment (1991), *J. Geophys. Res.*, *101*, 2025–2035, 1996.

Chan, C. Y., and L. Y. Chan, The effects of meteorology and air pollutant transport on ozone episodes at a subtropical coastal Asian city, Hong Kong, *J. Geophys. Res.*, *105*, 20,707–20,719, 2000.

Chan, L. Y., C. Y. Chan, and Y. Qin, Surface ozone pattern in Hong Kong, *J. Appl. Meteorol.*, *37*(10), 1151–1165, 1998a.

Chan, L. Y., H. Y. Liu, K. S. Lam, T. Wang, S. J. Oltmans, and J. M. Harris, Analysis of the seasonal behavior of tropospheric ozone at Hong Kong, *Atmos. Environ.*, *31*, 159–168, 1998b.

Chan, L. Y., C. Y. Chan, H. Y. Liu, S. Christopher, S. J. Oltmans, and J. M. Harris, A case study on the biomass burning in Southeast Asia and enhancement of tropospheric ozone over Hong Kong, *Geophys. Res. Lett.*, *27*, 1479–1483, 2000.

Chin, M., D. J. Jacob, J. W. Munger, D. D. Parrish, and B. G. Doddridge, Relationship of ozone and carbon monoxide over North America, *J. Geophys. Res.*, *99*, 14,565–14,573, 1994.

Crawford, J., et al., An assessment of ozone photochemistry in the extratropical western North Pacific: Impact of continental outflow during the late winter/early spring, *J. Geophys. Res.*, *102*, 28,469–28,488, 1997.

Davis, D., et al., Assessment of the ozone photochemistry tendency in the western North Pacific as inferred from PEM-West A observations during the fall of 1991, *J. Geophys. Res.*, *101*, 2111–2134, 1996.

Derwent, R. G., P. G. Simmonds, S. Seuring, and C. Cimmer, Observation and interpretation of the seasonal cycles in the surface concentrations of ozone and carbon monoxide at Mace Head, Ireland from 1990 to 1994, *Atmos. Environ.*, *32*, 144–157, 1998.

Harris, J. M., and J. D. W. Kahl, A descriptive atmospheric transport climatology for the Mauna Loa Observatory, using clustered trajectories, *J. Geophys. Res.*, *95*, 13,651–13,667, 1990.

Harris, J. M., and J. D. W. Kahl, Analysis of 10-day isentropic flow patterns for Barrow, Alaska: 1985–1992, *J. Geophys. Res.*, *99*, 25,845–25,855, 1994.

Harris, J. M., S. J. Oltmans, E. J. Diugokencky, P. C. Novelli, B. J. Johnson, and T. Mefford, An investigation into the source of the springtime tropospheric ozone maximum at Mauna Loa Observatory, *Geophys. Res. Lett.*, *25*, 1895–1898, 1998.

Hoell, J. M., D. D. Davis, S. C. Liu, R. E. Newell, H. Akimoto, R. J. McNeal, and R. J. Bendura, The Pacific Exploratory Mission-West Phase B: February–March 1994, *J. Geophys. Res.*, *102*, 28,223–28,240, 1997.

Jacob, D. J., J. A. Logan, and P. P. Mupti, Effects of rising Asian emissions on surface ozone in the United States, *Geophys. Res. Lett.*, *26*, 2175–2178, 1999.

Jaffe, D., et al., Transport of Asian air pollution to North America, *Geophys. Res. Lett.*, *26*, 711–714, 1999.

Kajii, Y., K. Someno, H. Tanimoto, J. Hirokawa, H. Akimoto, T. Katsuno, and J. Kawara, Evidence for the seasonal variation of photochemical activity of tropospheric ozone: Continuous observation of ozone and CO at Happo, Japan, *Geophys. Res. Lett.*, *25*, 3505–3508, 1998.

Kato, H., S. Fujita, and S. Nishinomiya, Mechanism of spring high oxidant episode: A meteorological analysis in and around the Hokuriku district, Japan, *Atmos. Environ., Part A*, *24*, 2023–2033, 1990.

Merrill, J. T., Atmospheric long range transport to the Pacific Ocean, in *Chemical Oceanography*, vol. 10, edited by J. P. Riley and R. Ducce, pp. 15–50, Academic, San Diego, Calif., 1989.

Moody, J. L., S. J. Oltmans, H. Levy II, and J. T. Merrill, Transport climatology of tropospheric ozone: Bermuda, 1988–1991, *J. Geophys. Res.*, *100*, 7179–7194, 1995.

Newell, R. E., E. V. Browell, D. D. Davis, and S. C. Liu, Western Pacific tropospheric ozone and potential vorticity: Implications for Asian pollution, *Geophys. Res. Lett.*, *24*, 2733–2736, 1997.

Ogawa, T., and A. Miyata, Seasonal variation of the tropospheric ozone: A summer minimum in Japan, *J. Meteorol. Soc. Japan*, *63*, 937–946, 1985.

Ogawa, T., and A. Miyata, Seasonal behavior of the tropospheric ozone in Japan, in *Atmospheric Ozone: Proceedings of the Quadrennial Ozone Symposium Held in Halkidiki, Greece, 3–7 Sept. 1984*, edited by C. S. Zerefos and A. Ghazi, D. Reidel, Norwell, Mass., 1989.

Oltmans, S. J., and H. Levy II, Seasonal cycle of surface ozone over the western North Atlantic, *Nature*, *358*, 392–394, 1992.

Parrish, D. D., J. S. Holloway, M. Trainer, P. C. Murphy, G. L. Forbes, and F. C. Fehsenfeld, Export of North American ozone pollution to the North Atlantic Ocean, *Science*, *259*, 1436–1439, 1993.

Parrish, D. D., M. Trainer, J. S. Holloway, J. E. Yee, M. S. Warshawaky, F. C. Fensenfeld, G. Forbes, and J. L. Moody, Relationships between ozone and carbon monoxide at surface sites in the North Atlantic region, *J. Geophys. Res.*, *103*, 13,357–13,367, 1998.

Piotrowicz, S. R., D. A. Boran, and C. J. Fisher, Ozone in the boundary layer of the equatorial Pacific Ocean, *J. Geophys. Res.*, *91*, 13,113–13,119, 1986.

Pochanart, P., J. Hirokawa, Y. Kajii, H. Akimoto, and M. Nakao, The influence of regional-scale anthropogenic activity in the northeast Asia on seasonal variations of surface ozone and its precursors observed at Oki, Japan, *J. Geophys. Res.*, *104*, 3621–3632, 1999.

Sunwoo, Y., G. R. Carmichael, and H. Ueda, Characteristics of background surface ozone in Japan, *Atmos. Environ.*, *28*, 25–37, 1994.

Talbot, R. W., et al., Chemical characteristics of continental outflow from Asia to the troposphere over the western Pacific Ocean during February–

March 1994: Results from PEM-West B, *J. Geophys. Res.*, *102*, 28,255–28,274, 1997.

Tsuruta, H., K. Shinya, T. Mizoguchi, and T. Ogawa, Seasonal behavior of the tropospheric ozone in rural Japan, in *Ozone in the Atmosphere*, edited by R. D. Bojkov and P. Fabian, pp. 433–436, A. Deepak, Hampton, Va., 1989.

Ueda, H., and G. R. Carmichael, Formation of secondary pollutants during long-range transport and its contribution to air quality in East Asia, *Terr. Atmos. Oceanic Sci. (TAO)*, *6*, 487–500, 1995.

Uematsu, M., R. A. Duce, J. M. Prospero, L. Chen, J. T. Merrill, and R. L. McDonald, Transport of mineral aerosol from Asia over the North Pacific Ocean, *J. Geophys. Res.*, *88*, 5343–5352, 1983.

Wang, T., K. S. Lam, L. Y. Chan, Z. L. Cheng, M. Anson, and M. A. Carroll, Trace gas measurement during the periods of outflow from the Asian continent: Results from a Hong Kong site during PEM-WEST B, *J. Geophys Res.*, *102*, 28,575–28,588, 1997.

Yienger, J. J., M. Galante, T. A. Holloway, M. J. Phadnis, S. K. Guttikunda, G. R. Carmichael, W. J. Moxim, and H. Levy II, The episodic nature of air pollution transport from Asia to North America, *J. Geophys. Res.*, *105*, 26,931–26,945, 2000.

C. Y. Chan, L. Y. Chan, K. S. Lam, and Y. S. Li, Environmental Engineering Unit, Department of Civil and Structural Engineering, Hong Kong Polytechnic University, Hung Hom, Hong Kong, China. (cececychan@polyu.edu.hk; celychan@polyu.edu.hk; cekslam@polyu.edu.hk; ceysli@polyu.edu.hk)

S. J. Harris and S. J. Oltmans, NOAA Climate Monitoring and Diagnostics Laboratory, 325 Broadway R/E/CG1, Boulder, CO 80305, USA. (jharris@cmdl.noaa.gov; soltmans@cmdl.noaa.gov)

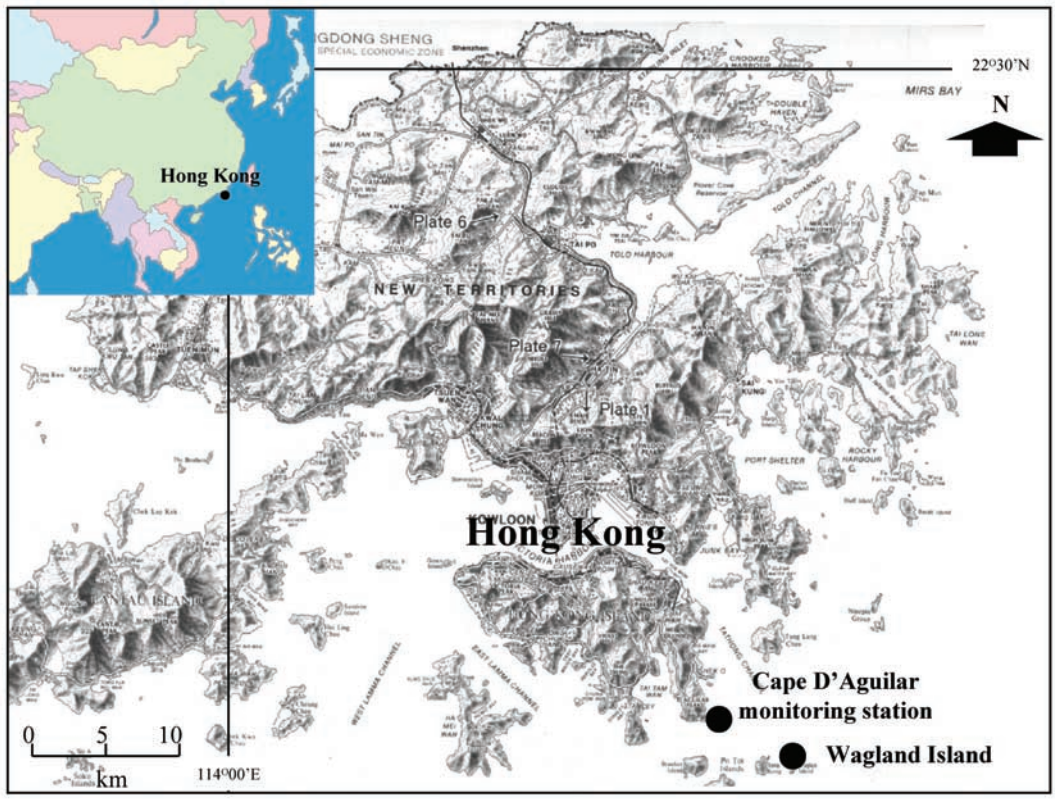

Figure 1. Geographical locations of Hong Kong and the Cape D'Aguilar monitoring station.

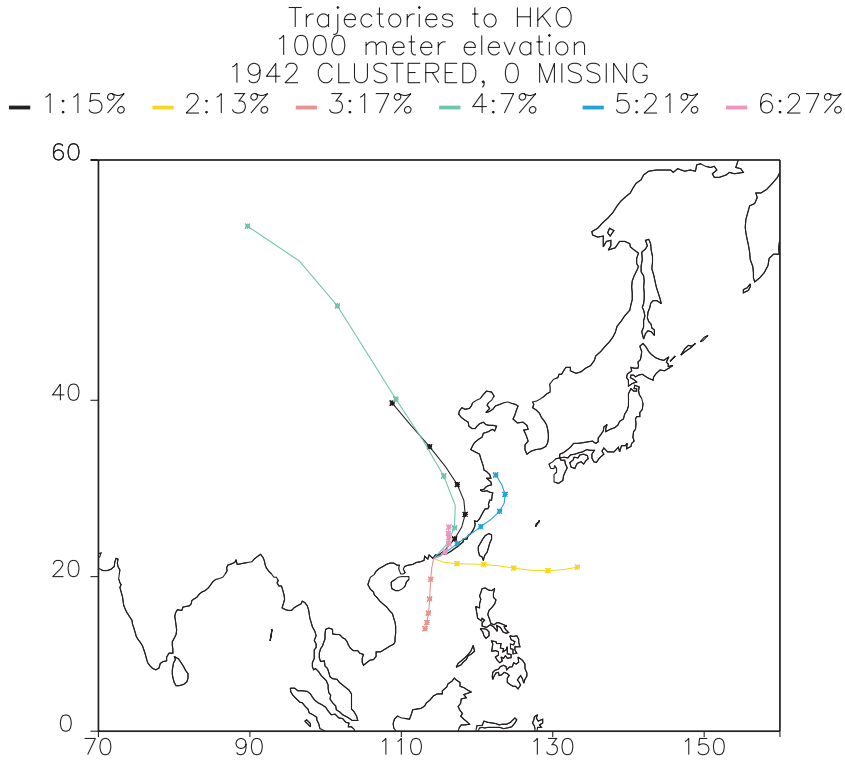

Figure 2. The six mean trajectory clusters arriving at Hong Kong.